Experimental Implementation of Efficient Quantum Pseudorandomness on a 12-Spin System

Jun Li,[1,2,3,4,*] Zhihuang Luo,[5,2,1] Tao Xin,[1,2,4] Hengyan Wang,[6] David Kribs,[7,3] Dawei Lu,[1,2,4,†] Bei Zeng,[2,3,7,‡] and Raymond Laflamme[3,8]

[1]*Shenzhen Institute for Quantum Science and Engineering, and Department of Physics, Southern University of Science and Technology, Shenzhen 518055, China*
[2]*Center for Quantum Computing, Peng Cheng Laboratory, Shenzhen 518055, China*
[3]*Institute for Quantum Computing, University of Waterloo, Waterloo N2L 3G1, Ontario, Canada*
[4]*Shenzhen Key Laboratory of Quantum Science and Engineering, Shenzhen 518055, China*
[5]*Laboratory of Quantum Engineering and Quantum Metrology, School of Physics and Astronomy, Sun Yat-Sen University (Zhuhai Campus), Zhuhai 519082, China*
[6]*Department of Physics, Zhejiang University of Science and Technology, Hangzhou 310023, China*
[7]*Department of Mathematics & Statistics, University of Guelph, Guelph N1G 2W1, Ontario, Canada*
[8]*Perimeter Institute for Theoretical Physics, Waterloo N2L 2Y5, Ontario, Canada*

(Received 7 August 2018; published 15 July 2019)

Quantum pseudorandomness, also known as unitary designs, comprises a powerful resource for emergent quantum technologies. Although in theory pseudorandom unitary operators can be constructed efficiently, realizing these objects in realistic physical systems is a challenging task. Here, we demonstrate experimental generation and detection of quantum pseudorandomness on a 12-qubit nuclear magnetic resonance system. We first apply random sequences to the interacting nuclear spins, leading to random quantum evolutions that can quickly form unitary designs. Then, in order to probe the growth of quantum pseudorandomness during the time evolutions, we propose the idea of using the system's multiple-quantum coherence distribution as an indicator. Based on this indicator, we measure the spreading of quantum coherences and find that substantial quantum pseudorandomness has been achieved at the 12-qubit scale. This may open up a path to experimentally explore quantum randomness on forthcoming large-scale quantum processors.

DOI: 10.1103/PhysRevLett.123.030502

Introduction.—Quantum randomness is a fundamental concept as well as a useful tool in many fields of modern quantum science and technology. In nonequilibrium statistical mechanics, random quantum processes play key roles in understanding many-body quantum systems out of equilibrium, as they capture universal properties of system dynamics and model the approach to thermalization [1–4]. In quantum computing, random transformations are crucial for demonstrating quantum advantages [5–7]. Recent progress in quantum information processing has further intrigued novel applications of quantum randomness. It is now widely used in quantum tomography [8,9], fidelity estimation [10], Rényi entropy measurement [11,12], and noise characterization [13–15]. For example, randomized benchmarking [14], as a standard technique for characterizing quantum devices, crucially relies on the ability to sample random quantum operations.

However, similarly to the classical case, the complexity of generating fully random transformations on a quantum system grows exponentially with the system size [16]. Therefore, quantum pseudorandomness, often cast as unitary designs, was proposed as an alternate. Unitary designs are operationally useful sets of unitaries. A k design is any ensemble of unitaries capable of simulating up to the kth order statistical moments of the Haar ensemble on average [17]. Great efforts were devoted to efficient constructions of k designs or explorations of their practical uses. Unfortunately, experimental progress is very limited—unitary designs have been achieved only in small-sized physical systems [18–20]. As the scale of controllable quantum systems is growing rapidly, realizing quantum pseudorandomness in these systems becomes an important task.

In this work, we realize experimental generation of approximate unitary 2-designs on a 12-qubit nuclear magnetic resonance (NMR) system. On the whole, our experimental implementation is based on addressing two key problems. The first problem concerns experimental feasibility of generating quantum pseudorandomness. There exist a variety of generation protocols, including polynomial-sized random quantum circuits [21–26], graph state techniques [27,28], and random dynamics of some design Hamiltonian [29], each with its own pros and cons. In practice, we follow the design Hamiltonian approach due to its advantages in saving qubit resources and in reducing time cost. A design Hamiltonian is some random

Hamiltonian satisfying that its time evolutions form unitary designs spontaneously. A concrete form of the design Hamiltonian was proposed in Ref. [29], which is composed of periodically changing random spin-glass-type interactions. In experiment, we show that these disordered interactions can be readily simulated by NMR refocusing techniques. Our numerical and experimental results demonstrate that, evolving the 12-qubit system under a suitably created design Hamiltonian is an effective way in producing pseudorandomness.

The second problem refers to the probe of generated randomness. Recent studies suggest that tools such as out-of-time-order correlators [29,30], Rényi entanglement entropies [12], or neural networks [31] may serve as diagnostics of unitary designs. However, there is much lesser experimental study due to the difficulty arising from the complexity in manipulating and detecting systems at scale. For instance, Ref. [30] showed that a natural probe of randomness, namely, *frame potential*, can be expressed in terms of out-of-time-order correlators. But these correlators become difficult to estimate at late times of the design Hamiltonian evolution, because they tend to be saturated to their corresponding Haar values, which are exponentially small in the system size. In fact, previous experiments measuring out-of-time-order functions were focused on the short-time decay part [32,33]. However, our study concerns both the short-time and long-time behavior of the pseudorandomness generation process, as the former features the convergence property and the latter signals the onset of pseudorandomness. For this purpose, we propose that the multiple-quantum coherence (MQC), a well-established technique from solid-state NMR [34,35], is a good indicator. Recently, MQCs found interesting applications in the studying of dynamical and statistical behavior of complex quantum systems, such as localization-delocalization transition [36–38], buildup of multiparticle entanglement [39], and information scrambling [32]. Here, we demonstrate that MQC spectra can also be used as a suitable means for detecting the time-development of pseudorandomness.

Definitions.—We briefly review the definitions of random unitary matrices and unitary designs. Let $\mathbb{U}(d)$ denote the group of $d \times d$ unitary matrices, and consider an ensemble of unitary operators $\mathcal{E} = \{U_i\}$ where $U_i \in \mathbb{U}(d)$. Let $\mathcal{E}_{\mathrm{Haar}}$ denote the ensemble of unitary matrices uniformly distributed with respect to the Haar measure on $\mathbb{U}(d)$. An ensemble $\mathcal{E}$ is said to be an approximate unitary design if it is close to the Haar ensemble $\mathcal{E}_{\mathrm{Haar}}$. More precisely, $\mathcal{E}$ forms an ϵ-approximate k design, if for every monomial $P(U) = U_{i_1 j_1} \cdots U_{i_k j_k} U^*_{m_1 n_1} \cdots U^*_{m_k n_k}$ of a degree not more than k, its average over $\mathcal{E}$ is ϵ close to that over the Haar ensemble $\mathcal{E}_{\mathrm{Haar}}$, i.e., $|(\mathbb{E}_{\mathcal{E}} - \mathbb{E}_{\mathcal{E}_{\mathrm{Haar}}})P(U)| \leq \epsilon$ [26].

Approximate unitary designs can be realized in a number of ways, among which the design Hamiltonian approach is relatively easier to implement experimentally. A design Hamiltonian is a physically local Hamiltonian whose interactions vary randomly at each time step, and its dynamics forms a unitary design after a threshold time [29]. Mathematically, an ϵ-approximate k-design Hamiltonian with l-local interaction is a random l-local Hamiltonian $\mathcal{H}$, where there exists $t_0 > 0$ such that, for most of the time $t \geq t_0$, the propagator $U(t) = \int_0^t \exp(-i\mathcal{H}s)ds$ is an ϵ-approximate unitary k design. Here, the shortest such time t_0 is called the design time of $\mathcal{H}(t)$.

Experimental scheme.—In experiment, we implement unitary 2-designs using the design Hamiltonian approach. In the following, we will focus on this concrete example to explain how to generate and probe quantum pseudorandomness. Our quantum processor is the home-prepared per-^{13}C-labeled dichlorocyclobutanone derivative, which contains 7 labeled carbon nuclei and 5 proton nuclei and hence forms a 12-qubit system; see Fig. 1(a). Experiments were carried out on a Bruker Avance III 700 MHz spectrometer at room temperature. The Hamiltonian and its parameters can be found in the Supplemental Materials [40].

To construct the design Hamiltonian proposed in Ref. [29], we apply a series of random refocusing pulse sequences as shown in Fig. 1(c). The refocusing sequences consist of a set of single-qubit π pulses about the x or y axis [41], and change-of-basis Hadamard operations $H^{\otimes n}$ in between. Here, randomness comes from the π rotations applied at random time, which is similar to the idea in constituting randomized dynamical decoupling protocols [42,43]. In experiment, the concrete form of the random refocusing sequence is as follows. We introduce a set of

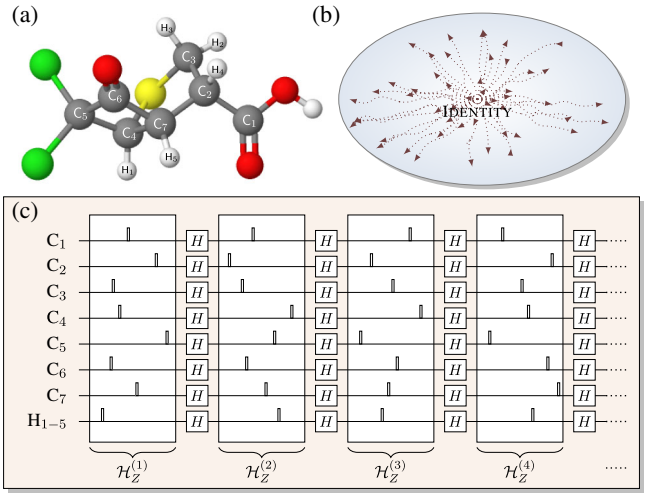

FIG. 1. (a) Molecular structure of per-^{13}C-labeled dichlorocyclobutanone. (b) Intuitive picture of time evolution operators generated by a design Hamiltonian. It starts from the identity, and approaches randomly distributed unitaries over the whole unitary group as time passes. The trajectories represent different time evolutions. (c) Schematic illustration of random refocusing sequences that are applied to our 12-qubit system to produce random Hamiltonian evolutions. The small rectangles represent single-qubit π rotations.

8-tuple column vectors $\lambda = \{\lambda^{(m)} : m = 1, 2, \ldots\}$. In Fig. 1(c), $m = 4$ blocks are plotted and the length for each block is fixed to be $T/2$. Each $\lambda^{(m)}$ contains eight entries randomly chosen from the unit interval to determine where to insert the π pulses, that is, the number $\lambda_i^{(m)}$ means a π pulse that is applied on the ith qubit in the mth block at time $\lambda_i^{(m)} T/2$. Hence, in each block, the corresponding dynamical evolution is governed by an effective disordered Hamiltonian

$$\mathcal{H}_Z^{(m)} = \sum_i \Omega_i^{(m)} \sigma_z^i + \sum_{i<j} J_{ij}^{(m)} \sigma_z^i \otimes \sigma_z^j, \tag{1}$$

where the frequencies $\Omega_i^{(m)}$ and the couplings $J_{ij}^{(m)}$ are randomly tuned by varying the locations of π pulses. The function of the n-fold Hadamard gate $H^{\otimes n}$ is to turn a Pauli-σ_z basis into a Pauli-σ_x basis. The essential idea is that, these alternate applications of time evolutions under dual bases enable a quick approach to quantum pseudorandomness.

It is necessary to check to what extent our Hamiltonian forms an approximate design Hamiltonian. A complete test for unitary designs is by frame potential [44]. Let $\mathcal{E} = \{U_i\}$ be an ensemble, the kth frame potential is defined as the average of the kth powers of the ensemble elements' Hilbert-Schmidt overlaps [45]

$$F_{\mathcal{E}}^{(k)} = \frac{1}{|\mathcal{E}|^2} \sum_{i,j} |\mathrm{Tr}(U_i U_j^\dagger)|^{2k}. \tag{2}$$

There is $F_{\mathcal{E}}^{(k)} \geq F_{\mathcal{E}_{\mathrm{Haar}}}^{(k)} = k!$, with equality if and only if $\mathcal{E}$ is a k design. Thus the deviation $F_{\mathcal{E}}^{(k)} - F_{\mathcal{E}_{\mathrm{Haar}}}^{(k)}$ can serve as a measure of how close $\mathcal{E}$ is to a k design. For large-sized systems $d \geq k$, $\mathcal{E}$ must contain an exponential number (at least $|\mathcal{E}| \geq d^{2k}/k!$) of unitaries to become a k design [46], implying that the exact frame potential calculation is intractable. In our 12-qubit case, we thus use statistical estimation and perform numerical simulation to compute the first and the second frame potentials. We statistically generate a sample of unitaries $\mathcal{E}$ based on our random Hamiltonian evolutions and observe the convergence of the frame potentials with respect to the sample size $|\mathcal{E}|$. Figure 2 shows our numerical results for different T. Obviously, for a range of T and after two rounds of evolutions, the estimated frame potentials converge to their corresponding Haar values. The simulation results present strong evidence that our design Hamiltonian can generate an ensemble of unitaries with significant amount of randomness.

Probing quantum pseudorandomness.—We perform MQC growth experiments to detect the generated quantum pseudorandomness. An outline of the experimental procedure is shown in Fig. 3(a). It contains four steps: (i) start from a simple initial state $\rho(0)$ (e.g., a localized state); (ii) evolve under our design Hamiltonian $\mathcal{H}$ to get

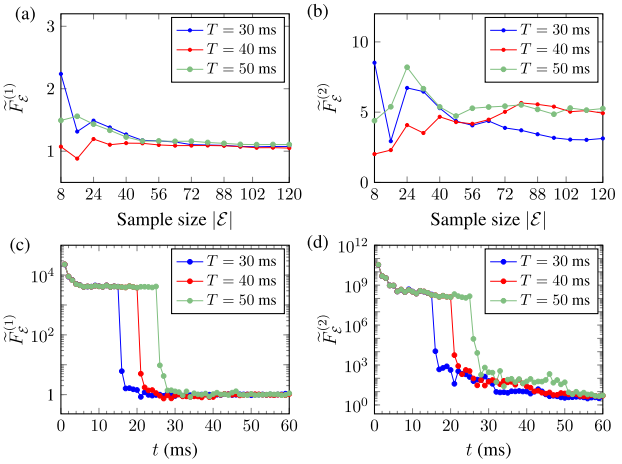

FIG. 2. Numerical simulation of the first and the second frame potentials of our design Hamiltonian's dynamics. (a),(b) The total evolution time is fixed as 60 ms, where a sampling of 120 evolutions almost achieves the convergence of $\tilde{F}_{\mathcal{E}}^{(k)}$. Here, $\tilde{F}_{\mathcal{E}}^{(k)}$ is equivalent to the frame potential in Eq. (2) up to a constant, so it exhibits the same tendency. It is used to make the simulation accessible for the case of 12 qubits; see details in the Supplemental Material [40]. (c),(d) We fix the sample size $|\mathcal{E}|$ to be 120. $\tilde{F}_{\mathcal{E}}^{(k)}$ drops abruptly when the change-of-basis operation $H^{\otimes n}$ is applied. As the evolution time grows, they eventually approach the corresponding Haar values, respectively.

$\rho(t) = e^{-i\mathcal{H}t} \rho(0) e^{i\mathcal{H}t}$; (iii) apply a collective rotational operator $\phi_z = e^{-iM_z\phi}$ with $M_z = \sum_i \sigma_z^i/2$; (iv) reverse the random evolution in the second step.

Let us explain the above four-step procedure. If the design Hamiltonian evolution $e^{-i\mathcal{H}t}$ is sufficiently random, it will excite all orders of coherences in $\rho(t)$ from a local operator $\rho(0)$. Here, for the basis $|i\rangle\langle j|$ in the Zeeman representation, a coherence order ν is the difference between two quantum numbers: $\nu = \langle i|M_z|i\rangle - \langle j|M_z|j\rangle$. So we expand $\rho(t) = \sum_\nu \rho_\nu(t)$, where $\rho_\nu(t)$ is the submatrix composed of all the order-ν elements. The core of the procedure is step (iii), that is, the coherence order information is encoded into the phase because $\phi_z \rho_\nu(t) \phi_z^\dagger = e^{-i\nu\phi} \rho_\nu(t)$. Finally, we reverse the random evolution and measure the overlap $S(\phi, t)$ between the final state and the initial state, which gives

$$S(\phi, t) = \sum_\nu e^{-i\nu\phi} I(\nu, t). \tag{3}$$

Here $I(\nu, t) = \mathrm{Tr}[\rho_\nu^2(t)]$ is the amplitude for a given order ν. Now it is clear that the steps taken above are to ensure that in observing the multiple-quantum signal, all contributions to a given order of coherence are generated with the same phase. We then measure $S(\phi, t)$ as a function of ϕ at a fixed time t and then perform the Fourier transform with respect to ϕ. This gives all the amplitudes $I(\nu, t)$ of $\rho(t)$ and hence the MQC spectrum is obtained. Furthermore, by varying the evolution time t, we see the growth of MQCs.

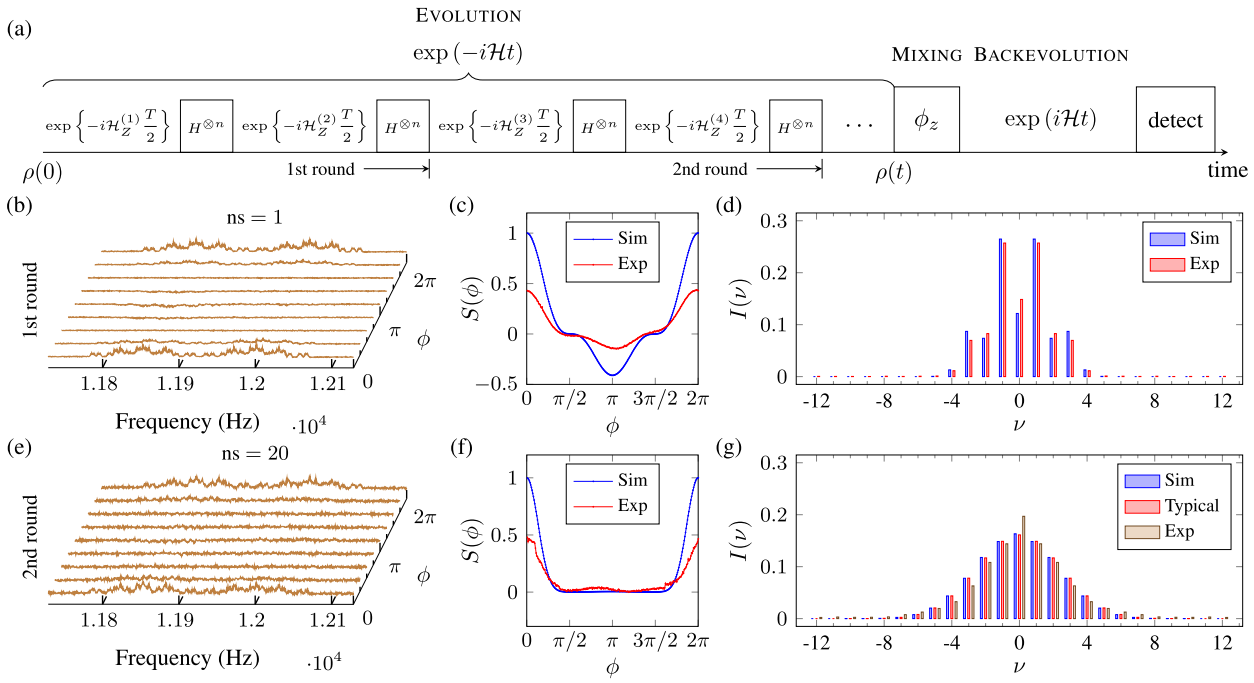

FIG. 3. (a) Experimental sequence for measuring the MQC spectra. The two rounds of the design Hamiltonian evolution and the reverse correspond to sequence lengths of 34 ms and 42 ms, respectively. All the π rotations and Hadamard gates cost 2 ms. (b)–(g) Experimentally measured MQCs of the evolved state $\rho(t)$ at the first round (b)–(d) and the second round (e)–(g) of the design Hamiltonian evolution. (b),(e) A chosen set of experimental C_7 spectra. Here, ns means the number of scans that we repeat the experiment to gain a good signal. (c),(f) Multiple-quantum signals observed at varying rotational angles ϕ. The left-right asymmetry is due to the imperfect time reversal of the dynamics. (d),(g) Profiles for the MQC spectral intensity. The intensity for each order is normalized relative to the total spectral intensity. It can be seen that the MQCs generated in experiment rapidly spread over the system's degrees of freedom.

The next question is how $I(\nu, t)$ is distributed when the evolution $e^{-i\mathcal{H}t}$ is truly random. We conclude that the typical distribution shows a Gaussian pattern $I_{\text{typical}}(\nu) \sim \exp(-\nu^2/n)$, where n is the number of qubits. The reason is as follows. Under a Haar random operation, all possible coherences will be excited with equal probability. Therefore, the total intensity within a given order ν simply relies on the number of transitions consistent with that order. In an n-spin system, the number of configurations for any coherence order ν is $[(2n)/(n-\nu)]$, which is well approximated by $2^{2n}(n\pi)^{-1/2}\exp(-\nu^2/n)$ for $n > 6$. So in our case that $n = 12$, the resulting MQC spectrum typically shows a Gaussian pattern. These results can be derived from evaluating moments of polynomials on random unitaries [47]; see more details in the Supplemental Material [40]. The behavior has been observed in solid-state NMR where the spin dynamics is rather complex [34,35]. Accordingly, we expect in experiment that at long time t,

$$I(\nu, t) \to I_{\text{typical}}(\nu). \tag{4}$$

In other words, the essential idea for probing the onset of quantum pseudorandomness is to measure the MQC spectrum, and then compare it with $I_{\text{typical}}(\nu)$.

Figure 3 shows the experimentally extracted MQC distributions in our 12-qubit system at the first and second round of the design Hamiltonian evolution. Here, the initial state is chosen as $\rho(0) = \sigma_z^7$ with $T = 30$ ms. The positions of the π pulses, determined by the randomly generated array λ, are given in the Supplemental Material [40]. The π rotations and Hadamard gates are realized by 2 ms shaped pulses, which are obtained using the scalable pulse compiler technique [48,49]. Their simulated fidelities are all above 98.5%. Pulse imperfections and the decoherence effect accumulated over the two rounds of evolution are the primary error sources, which reduce the signal-to-noise ratio in multiple-quantum signals as high-order coherences are extremely fragile. Even though, a spreading tendency for higher-order coherences is clearly evident in the spectra as shown in Figs. 3(d) and 3(g). In particular, we put the typical MQC profile $I_{\text{typical}}(\nu)$ in Fig. 3(g) for comparison, which is in good agreement with the experimental result. Thus, the experimentally observed redistribution of spectral intensity into high-order coherences is a tangible manifestation of the growth of quantum pseudorandomness during the evolution period.

Discussion.—To generate sufficiently random quantum processes on a real system requires extensive control over the system's degrees of freedom. The NMR platform is well

suited to study pseudorandomness generation process; e.g., the mature MQC technique considerably assists in probing the amount of randomness. Thus it is an excellent test bed to realize relevant ideas. Our experimental results demonstrate that the practical realization of pseudorandom operators is possible via random control sequences with reasonable lengths. In particular, there is no need to perform coupled operations between physically nonadjacent spins, and no fine control of the evolution time is required. However, a major challenge left open is to quantify the effect of decoherence and control imperfections. Future work will analyze such issues to gain a better understanding of the experimental reliability of the design Hamiltonian approach.

As to the applications of quantum pseudorandomness, a practical pseudorandomness generator is undoubtedly an important tool for emerging quantum technologies. Apart from its vast applications in quantum information science, generating random quantum processes also benefits many other fields in quantum physics, e.g., the study of thermalization in isolated quantum systems. In the current framework of investigating thermalizing behaviors, such as information scrambling [2,3,50], operator spreading [51,52], and entanglement growth [53,54], randomness continuously plays a prominent role. These novel theories will be subject to experimental examinations once high-dimensional random processes can be made accessible in practice. In this sense, our work involving 12 qubits takes a step towards building pseudorandomness generators at scale. Two accompanying difficulties, the generation and detection of quantum pseudorandomness, have been overcome by employing the scalable design Hamiltonian approach and the MQC indicator, respectively. Because of the wide applicability of quantum pseudorandomness, we anticipate the techniques developed and demonstrated here to find broader applications in future quantum tasks.

We are grateful to the following funding sources: NSERC (D. K., B. Z., and R. L.); CIFAR (B. Z. and R. L.). J. L., T. X., and D. L. are supported by the National Natural Science Foundation of China (Grants No. 11605005, No. 11875159, and No. U1801661), Science, Technology and Innovation Commission of Shenzhen Municipality (Grants No. ZDSYS20170303165926217, No. JCYJ20170412152620376, and No. JCYJ20180302174036418), Guangdong Innovative and Entrepreneurial Research Team Program (Grant No. 2016ZT06D348).

*lij3@sustech.edu.cn
†ludw@sustech.edu.cn
‡zengb@uoguelph.ca

[1] J. Eisert, M. Friesdorf, and C. Gogolin, Nat. Phys. **11**, 124 (2015).
[2] D. A. Roberts and B. Yoshida, J. High Energy Phys. 04 (2017) 121.
[3] J. Cotler, N. Hunter-Jones, J. Liu, and B. Yoshida, J. High Energy Phys. 11 (2017) 48.
[4] P. Kos, M. Ljubotina, and T. Prosen, Phys. Rev. X **8**, 021062 (2018).
[5] M. A. Broome, A. Fedrizzi, S. Rahimi-Keshari, J. Dove, S. Aaronson, T. C. Ralph, and A. G. White, Science **339**, 794 (2013).
[6] J. B. Spring, B. J. Metcalf, P. C. Humphreys, W. S. Kolthammer, X.-M. Jin, M. Barbieri, A. Datta, N. Thomas-Peter, N. K. Langford, D. Kundys, J. C. Gates, B. J. Smith, P. G. R. Smith, and I. A. Walmsley, Science **339**, 798 (2013).
[7] M. Oszmaniec, R. Augusiak, C. Gogolin, J. Kołodyński, A. Acín, and M. Lewenstein, Phys. Rev. X **6**, 041044 (2016).
[8] I. Roth, R. Kueng, S. Kimmel, Y.-K. Liu, D. Gross, J. Eisert, and M. Kliesch, Phys. Rev. Lett. **121**, 170502 (2018).
[9] L. Banchi, W. S. Kolthammer, and M. S. Kim, Phys. Rev. Lett. **121**, 250402 (2018).
[10] C. Dankert, R. Cleve, J. Emerson, and E. Livine, Phys. Rev. A **80**, 012304 (2009).
[11] A. Elben, B. Vermersch, M. Dalmonte, J. I. Cirac, and P. Zoller, Phys. Rev. Lett. **120**, 050406 (2018).
[12] Z.-W. Liu, S. Lloyd, E. Y. Zhu, and H. Zhu, Phys. Rev. Lett. **120**, 130502 (2018).
[13] J. Emerson, R. Alicki, and K. Życzkowski, J. Opt. B **7**, S347 (2005).
[14] J. Emerson, M. Silva, O. Moussa, C. Ryan, M. Laforest, J. Baugh, D. G. Cory, and R. Laflamme, Science **317**, 1893 (2007).
[15] E. Magesan, J. M. Gambetta, and J. Emerson, Phys. Rev. Lett. **106**, 180504 (2011).
[16] M. Pozniak, K. Zyczkowski, and M. Kus, J. Phys. A **31**, 1059 (1998).
[17] C. Dankert, R. Cleve, J. Emerson, and E. Livine, Phys. Rev. A **80**, 012304 (2009).
[18] J. M. Chow, J. M. Gambetta, L. Tornberg, J. Koch, L. S. Bishop, A. A. Houck, B. R. Johnson, L. Frunzio, S. M. Girvin, and R. J. Schoelkopf, Phys. Rev. Lett. **102**, 090502 (2009).
[19] A. D. Córcoles, J. M. Gambetta, J. M. Chow, J. A. Smolin, M. Ware, J. Strand, B. L. T. Plourde, and M. Steffen, Phys. Rev. A **87**, 030301(R) (2013).
[20] J. C. F. Matthews, R. Whittaker, J. L. O'Brien, and P. S. Turner, Phys. Rev. A **91**, 020301 (2015).
[21] J. Emerson, Y. S. Weinstein, M. Saraceno, S. Lloyd, and D. G. Cory, Science **302**, 2098 (2003).
[22] L. Arnaud and D. Braun, Phys. Rev. A **78**, 062329 (2008).
[23] A. Harrow and R. A. Low, Commun. Math. Phys. **291**, 257 (2009).
[24] W. G. Brown and L. Viola, Phys. Rev. Lett. **104**, 250501 (2010).
[25] P. Ćwikliński, M. Horodecki, M. Mozrzymas, Ł. Pankowski, and M. Studziński, J. Phys. A **46**, 305301 (2013).
[26] F. G. S. L. Brandão, A. W. Harrow, and M. Horodecki, Phys. Rev. Lett. **116**, 170502 (2016).
[27] P. S. Turner and D. Markham, Phys. Rev. Lett. **116**, 200501 (2016).

[28] R. Mezher, J. Ghalbouni, J. Dgheim, and D. Markham, Phys. Rev. A **97**, 022333 (2018).
[29] Y. Nakata, C. Hirche, M. Koashi, and A. Winter, Phys. Rev. X **7**, 021006 (2017).
[30] D. A. Roberts and B. Yoshida, J. High Energy Phys. 04 (2017) 121.
[31] D. W. F. Alves and M. O. Flynn, arXiv:1808.10498v1.
[32] M. Gärttner, J. G. Bohnet, A. Safavi-Naini, M. L. Wall, J. J. Bollinger, and A. M. Rey, Nat. Phys. **13**, 781 (2017).
[33] J. Li, R. Fan, H. Wang, B. Ye, B. Zeng, H. Zhai, X. Peng, and J. Du, Phys. Rev. X **7**, 031011 (2017).
[34] J. Baum, M. Munowitz, A. N. Garroway, and A. Pines, J. Chem. Phys. **83**, 2015 (1985).
[35] S. Lacelle, Adv. Magn. Opt. Reson. **16**, 173 (1991).
[36] G. A. Álvarez and D. Suter, Phys. Rev. Lett. **104**, 230403 (2010).
[37] G. A. Álvarez, D. Suter, and R. Kaiser, Science **349**, 846 (2015).
[38] K. X. Wei, C. Ramanathan, and P. Cappellaro, Phys. Rev. Lett. **120**, 070501 (2018).
[39] M. Gärttner, P. Hauke, and A. M. Rey, Phys. Rev. Lett. **120**, 040402 (2018).
[40] See Supplemental Material at http://link.aps.org/supplemental/10.1103/PhysRevLett.123.030502 for molecular information, derivation of typical MQC distribution, additional simulations, and more experimental results.
[41] L. M. K. Vandersypen and I. L. Chuang, Rev. Mod. Phys. **76**, 1037 (2005).
[42] L. F. Santos and L. Viola, Phys. Rev. Lett. **97**, 150501 (2006).
[43] L. F. Santos and L. Viola, New J. Phys. **10**, 083009 (2008).
[44] J. M. Renes, R. Blume-Kohout, A. J. Scott, and C. M. Caves, J. Math. Phys. **45**, 2171 (2004).
[45] A. J. Scott, J. Phys. A **41**, 055308 (2008).
[46] A. Roy and A. J. Scott, Des. Code Cryptogr. **53**, 13 (2009).
[47] B. Collins, Int. Math. Res. Not. **2003**, 953 (2003).
[48] C. A. Ryan, C. Negrevergne, M. Laforest, E. Knill, and R. Laflamme, Phys. Rev. A **78**, 012328 (2008).
[49] J. Li, J. Cui, R. Laflamme, and X. Peng, Phys. Rev. A **94**, 032316 (2016).
[50] H. Gharibyan, M. Hanada, S. H. Shenkera, and M. Tezuka, J. High Energy Phys. 07 (2018) 124.
[51] A. Nahum, S. Vijay, and J. Haah, Phys. Rev. X **8**, 021014 (2018).
[52] V. Khemani, A. Vishwanath, and D. A. Huse, Phys. Rev. X **8**, 031057 (2018).
[53] A. Nahum, J. Ruhman, S. Vijay, and J. Haah, Phys. Rev. X **7**, 031016 (2017).
[54] C. W. von Keyserlingk, T. Rakovszky, F. Pollmann, and S. L. Sondhi, Phys. Rev. X **8**, 021013 (2018).